Supporting Information

Functionally modified TiO_2 nanoparticles with UV/pH dual-response for controllable emulsion separation

Yu-Ping Zhang[1,2]*, Chang-Hua Zhao[2] , Sheng-Qiang Qiu[a], Rui Ding[a] and Pei Yuan[a]

[1]College of Chemistry and Materials Engineering, Hunan University of Arts and Science, Changde, 415000, P.R. China

[2]College of Chemistry, Zhengzhou University, Zhengzhou 450001, P.R.China

Chemicals

TiO_2 (25 nm), Span 80, n-hexane (> 98%), iso-octane (> 99%), NaOH (96%), Methylene blue (MB) and petroleum ether (98%) were purchased from Shanghai Aladdin Biochemical Technology Co. CCl_4 (98%) was purchased from Shanghai Myriad. Toluene (AR) was purchased from Tianjin Fuyu Fine Chemical Co., Ltd, $HS(CH_2)_{11}CH_3$ (99%) was supplied by Shanghai Titan Technology Co., Ltd, $HS(CH_2)_{10}COOH$ (95%) was supplied by Shanghai McLean Biochemical Co., Ltd, $AgNO_3$ (AR) was purchased from Sinopharm Chemical Reagent Co.

Preparation of smart nanoparticles with dual response

To prepare Ag-modified TiO_2 nanoparticles (Ag@TiO_2), 0.3 g of TiO_2 (25 nm) was added to a 100 mL solution of 0.5 mM $AgNO_3$. The mixture was stirred in darkness for 30 min and then immediately transferred to a UV crosslinker. It was irradiated with five 365 nm UV lamps (power of 10 W, 8 cm from the liquid surface) for 10 min, during which the solution was stirred 3 to 5 times with a glass rod to ensure uniform illumination. The solution was then washed several times with deionized water and dried.

The prepared Ag@TiO_2 nanoparticles was immersed in a 30 mL ethanol solution containing $HS(CH_2)_{11}CH_3$ and $HS(CH_2)_{10}COOH$ (total concentration of 10 mM/L, with varying proportions of the two molecules) under dark conditions for more than 12 h. The powder was then washed several times with ethanol, and dried, to obtain the smart responsive TiO_2nps. The operational process was illustrated in **Fig.S1**.

Emulsion separation

Different types of oil/water mixture were prepared by dropping a small amount of oils or organic solvents (n-hexane, isooctane, petroleum ether, toluene, CCl_4) on the water surface. The involved organic solvents were dyed by Sudan III. The initially added TiO_2nps denoted as m_0 , and after the TiO2nps with complete adsorption of the oil were extracted for weighing, recorded as m_1. The adsorption capacity was calculated by equation (1) :

$$Q = \frac{m_1 - m_0}{m_0} \quad (1)$$

A stable O/W emulsion containing surfactant was obtained by mixing 0.1 g of Span 80 into a mixture of water and oil (n-hexane, iso-octane, petroleum ether, toluene, CCl_4) in a volume ratio of 99:1, followed by high-speed homogenization at 5000 r/min for 5 min. Various quantities of particles ranging from 20 to 80 mg were introduced into 5 mL of the O/W emulsion, followed by vortex shaking for 5 min to determine the minimum particle mass that completely absorbed oil droplets. Subsequently, the solution before and after adsorption treatment were observed and measured using an optical microscope and a particle size analyzer. Similarly, a stable W/O emulsion containing surfactant was obtained by mixing 0.1 g of Span 80 into a mixture of water and oil (n-hexane, iso-octane, petroleum ether, toluene, CCl_4) in a volume ratio of 1:99, followed by high-speed homogenization at 5000 r/min for 5 min. Different masses of hydrophilic particles (20-80 mg, treated with water at pH = 13 for 1 min and dried) were added to 5 mL of the W/O emulsion, followed by vortex shaking for 5 min to determine the minimum particle mass that completely absorbed water droplets. Subsequently, the solution before and after adsorption treatment were observed using an optical microscope and a particle size analyzer. The separation efficiency was calculated using Equation (2)：

$$R = \frac{C_0 - C_1}{C_0} \times 100\ \% \quad (2)$$

Where C0 and C1 (mg/L) are the oil (water) concentration in the oil-water emulsion before and after separation.Water (oil) concentration was determined using a Karl Fischer moisture analyzer (FK-WS1, Shan Dong Fangke Instrument Co., Ltd.) and a UV-Vis analyzer, respectively.

Characterization

The microstructure of the materials was analyzed using a transmission electron microscope (TEM, JEOL−JEM，2100F, Japan). Fourier transform infrared (FTIR) spectra were recorded on a Thermo Scientific Nicolet iS5 spectrometer (Thermo Fisher Scientific, USA) equipped with a KBr beam splitter optimized for the mid-infrared region. X-ray diffraction (XRD) patterns were acquired using a DX-2700 X-ray diffractometer (Haoyuan Instrument, Dandong, China). The measurements were performed in step-scan mode with a scanning range of 5°–80° (2θ), a step size of 0.025°, and a sampling time of 0.3 s per step. The X-ray tube was operated at a voltage of 30 kV and a current of 30 mA. The UV cross-linking instrument (SZ03−II, China) was used to complete the UV irradiation reduction experiments. Additionally, UV-VIS-NIR spectrophotometry (PE 750s, China) and Karl Fischer moisture titrator (FK-WS1, China) were used to detect oil and water concentrations before and after the separation of different emulsions. The optical microscopy (NOVEL NE 620, China) and dynamic light scattering (DLS, Zetasizer Nano ZSE, UK) were utilized for analyzing and observing emulsions before and after separation. The wetting properties of the materials were measured using an optical contact angle measurement instrument (TST-300H, China).

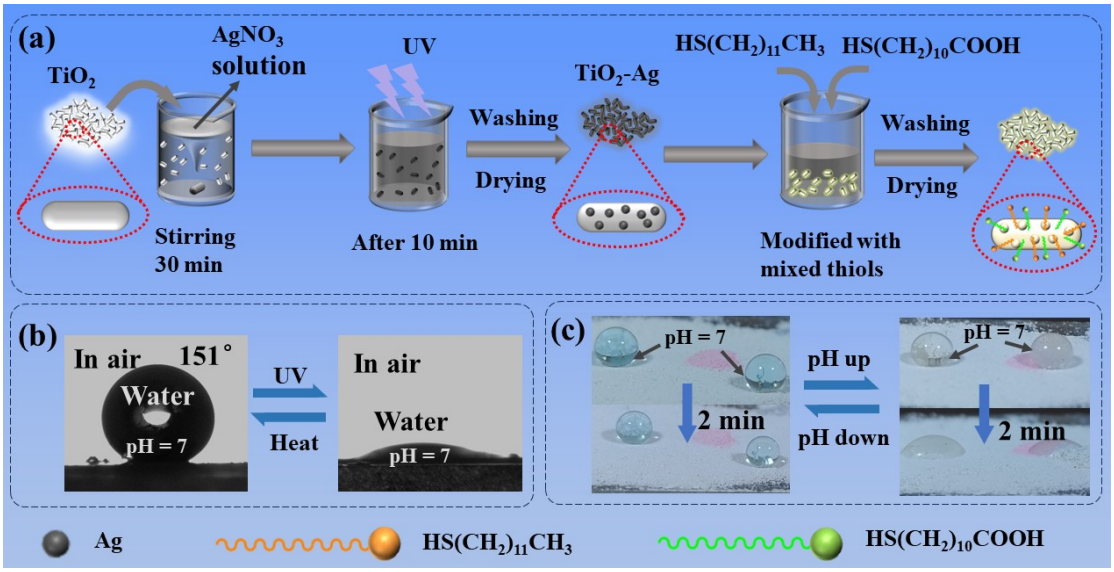

Fig.S1 The schematic diagram of preparation process and visual dual response of UV and pH. (a) Preparation for the smart TiO_2 nanoparticles with dual response; (b) reversibly switchable wettability with the help of UV irradiation and heat treatment; (c) reversibly switchable wettability under different pH conditions.

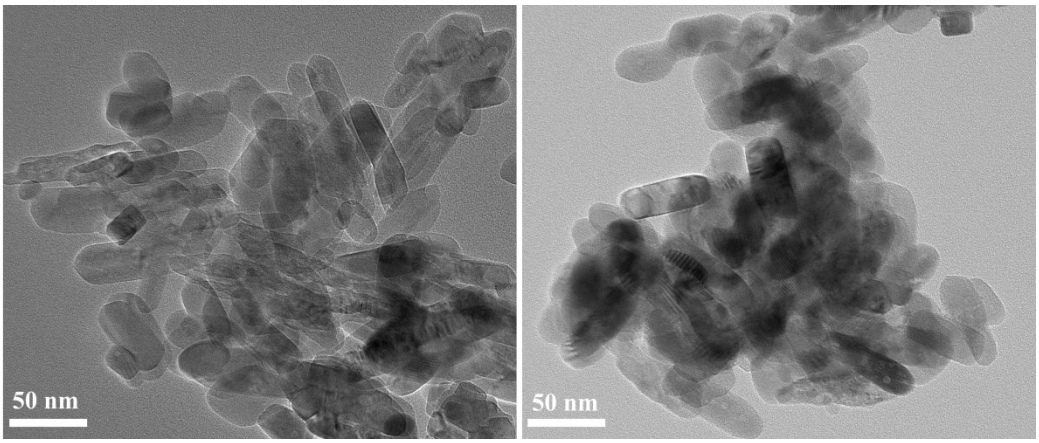

Fig. S2 TEM images of TiO_2 (left) and the as-prepared smart response nanoparticles (right).

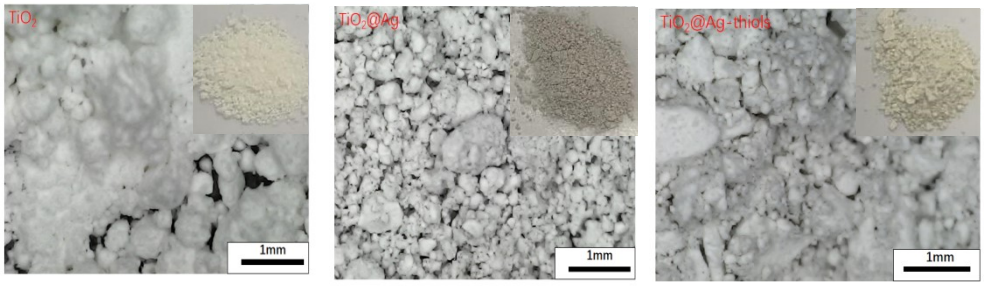

Fig. S3 Images of TiO_2 , TiO_2@Ag and TiO_2@Ag-thiols by electron microscope and apple phone (inlet).

FTIR spectra further characterize the surface functional group evolution of the as-prepared samples. Pure TiO_2 exhibits prominent absorption bands at 3430 cm^{-1} assigned to O-H stretching vibration and 1630 cm^{-1} corresponding to H-O-H bending vibration of adsorbed water. The FTIR profile of TiO_2@Ag is almost identical to that of pristine TiO_2 ,indicating that Ag introduction merely occurs via physical surface deposition without changing the surface chemical environment. By contrast, the TiO_2@Ag-thiols particles emerges new absorption peaks at 2920/2850 cm^{-1} and 1710 cm^{-1} , which are attributed to the stretching vibrations of alkyl -CH_2-/-CH_3 groups and C=O groups, respectively. In addition, the peak intensities at 3430 cm^{-1} and 1630 cm^{-1} are obviously attenuated, further confirming the successful grafting of thiol molecules and the decreased hydrophilicity of the material surface. XRD results demonstrate that all samples of TiO_2, TiO_2@Ag and TiO_2@Ag-thiols well match the standard anatase TiO_2 phase. No obvious displacement or morphological variation of diffraction peaks is observed among these samples, verifying that Ag deposition and subsequent thiol functionalization hardly affect the crystalline phase and lattice structure of the TiO_2 substrate. The absence of characteristic diffraction signals for metallic Ag implies that Ag nanoparticles are highly dispersed on the TiO_2 surface with a relatively low loading content.

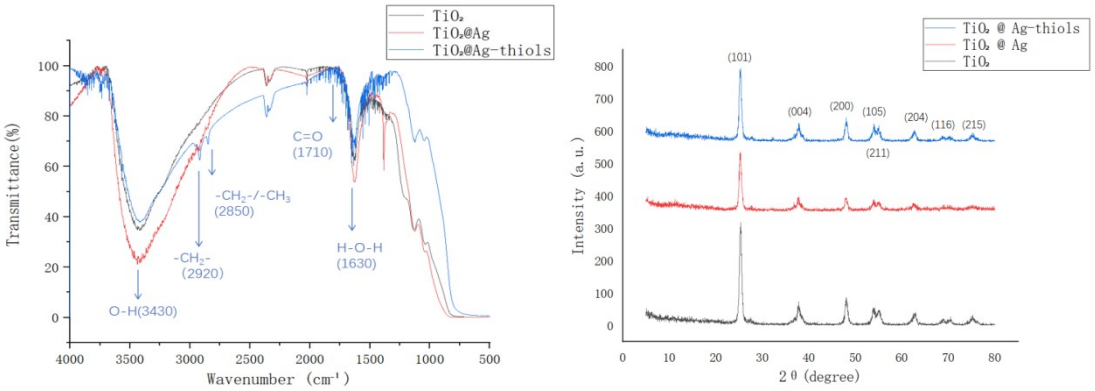

Fig. S4 Characterization of FTIR and XRD for the particles of TiO_2, TiO_2@Ag and TiO_2@Ag-thiols .

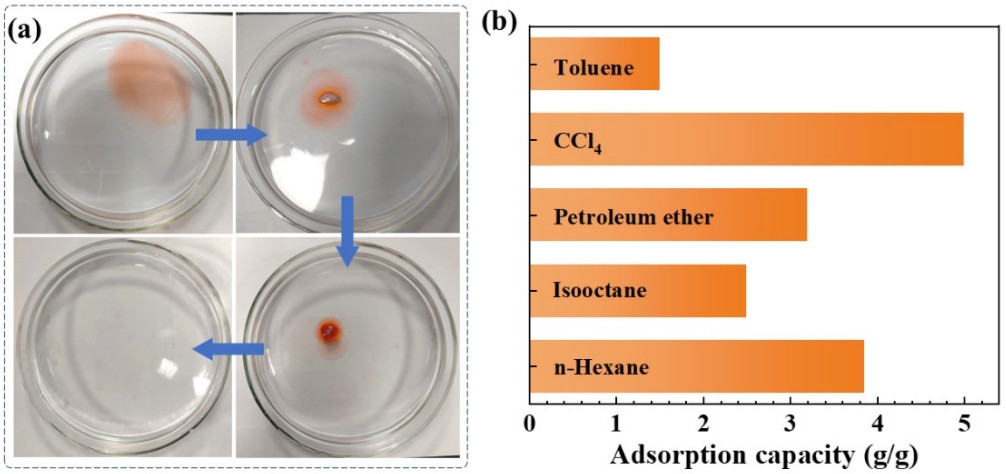

Fig. S5 (a) Smart nanoparticles used to collect red-dyed n-hexane on water surface; (b) oil absorption capacity of the smart superhydrophobic nanoparticles.

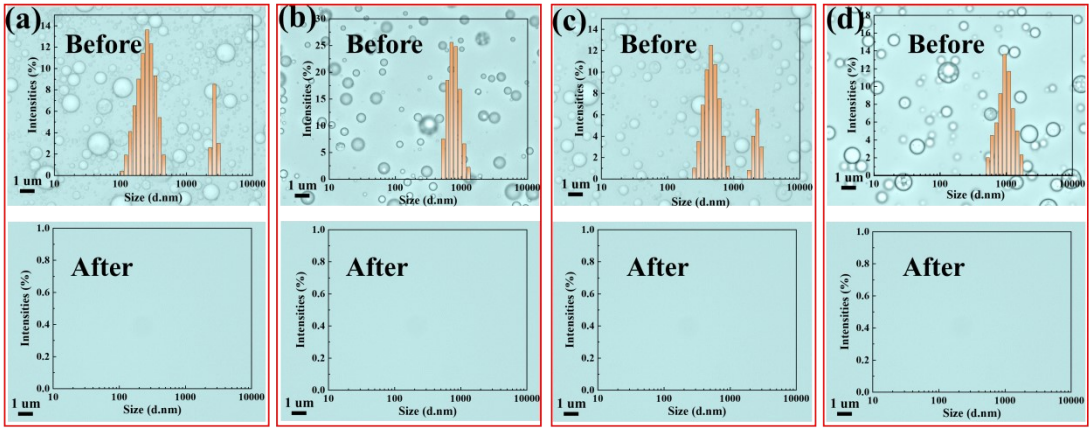

Fig.S6 PSD analysis of different O/W emulsions before and after separation.

Symbols a, b, c and d are the O/W emulsions of CCl_4-in-water, isooctane-in-water, PE-in-water and toluene-in-water, respectively.

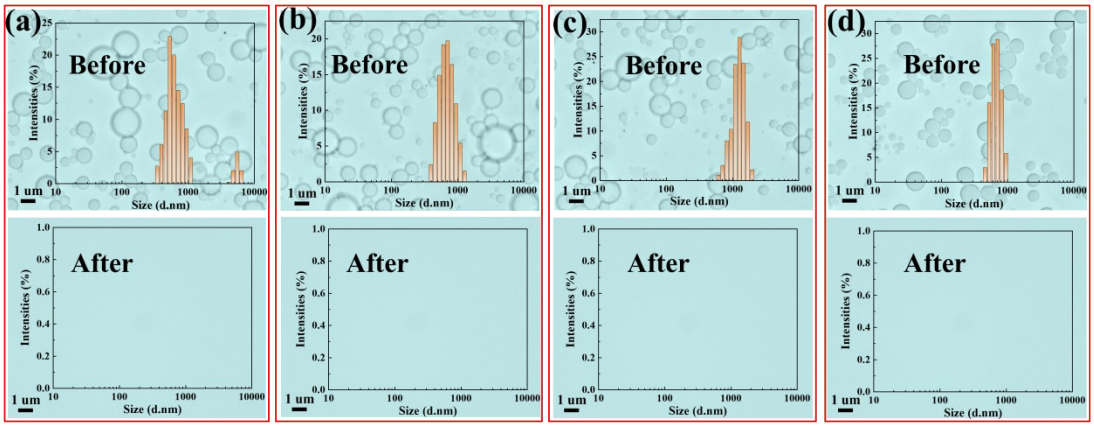

Fig.S7 PSD analysis of different W/O emulsions before and after separation.

Symbols a, b, c and d are the W/O emulsions of water-in-n-hexane, water-in-isooctane, water-in-PE and water-in-toluene.

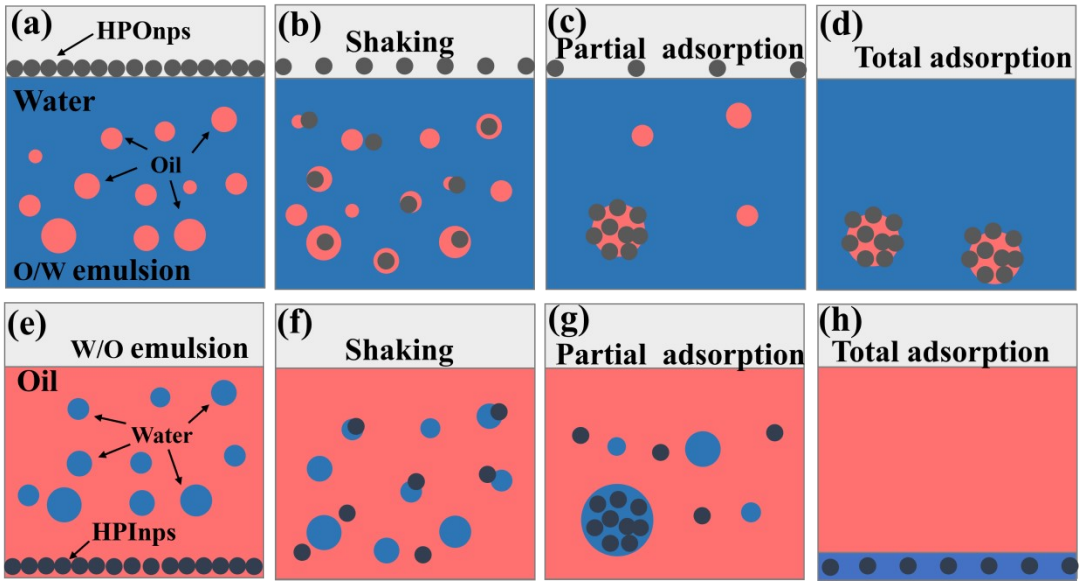

Fig. S8 Emulsion breaking diagrams for O/W and W/O emulsions

Table S1 Comparative separation performance for different adsorption particles.

Sorbent	WCA(◦)	Oil/organic solvent sorption type(s)	Sorption capacity (g/g)	Ref.
Cenospheres @ fluorocarbon resin @$CaCO_3$@SiO_2	153.3	n-Hexane, Diesel, Soybean oil, Petroleum ether, Dichloromethane	0.47−0.56	[1]
ZIF-8	142	Hexadecane, Dodecane Methanol, Dodecane, Tetradecane, Silicone oil, Dimethylformamide, Toluene, Chloroform, Dichloromethan	0.7–2.5	[2]
Iron particles	164	Xylene, kerosene, silicone oil, hexadecane, corn oil	0.28-0.45	[3]
Spiky nickel nanowires	169.2	Hexane, Heptane, Dodecane, Xylene, Gasoline, Ethyl acetate, Dimethylformamide, Corn oil, Sesame oil, Olive oil	3.86−5.27	[4]
Silk fibroin/chitosan/sodium stearate	143.3	Soybean oil, Engine oil	5.4−5.6	[5]
Fe_3O_4@DMONs	155.3	Petroleum ether, n-Hexane, n-Octane, Cyclohexane	1.37−2.04	[6]
Zinc oxide flower-like micro-particles	154	maize oil	0.5	[7]
Smart TiO_2nps	152	Toluene, Petroleum ether, CCl_4, Isooctane, n-Hexane	1.5−5	This work

Notes and references

1 G. X. Zhu, X. Li and X. Zhang, *Colloids Surf., A*, 2024, 681, 132811–132822.

2 E. E. Sann, Y. Pan, Z. F. Gao, S. S. Zhan and F. Xia, *Sep. Purif. Technol.*, 2018, 206, 186–191.

3 C. T. Duan, T. Zhu, J. Guo et al., *ACS Appl. Mater. Interfaces*, 2015, 7, 10475–10481.

4 H. Shayesteh, A. Rahbar-Kelishami and R. Norouzbeigi, *Ceram. Int.*, 2022, 48, 10999–11008.

5 X. Han, Y. Ke, Y. Wu, J. Huang, W. Xu and Y. Wang, *Powder Technol.*, 2023, 420.

6 B. Wang, Y. Wei, Q. Wang, J. Di, S. Miao and J. Yu, *Mater. Chem. Front.*, 2020, 4, 2184–2191.

7 C. Yang, X. Huang, Q. Jin et al., *Nanotechnology*, 2020, 31, 095712.